Grid Frequency Extreme Event Analysis and Modeling

Preprint

Maria Folgueras, Erin Wenger, Anthony Florita, Kara Clark, and Vahan Gevorgian
National Renewable Energy Laboratory

Presented at the International Workshop on Large-Scale Integration of Wind Power into Power Systems as well as on Transmission Networks for Offshore Wind Power Plants (Wind Integration Workshop)
Berlin, Germany
October 25–27, 2017

NREL is a national laboratory of the U.S. Department of Energy
Office of Energy Efficiency & Renewable Energy
Operated by the Alliance for Sustainable Energy, LLC

This report is available at no cost from the National Renewable Energy Laboratory (NREL) at www.nrel.gov/publications.

Conference Paper
NREL/CP-5D00-70029
November 2017

Contract No. DE-AC36-08GO28308

NOTICE

This report is available at no cost from the National Renewable Energy Laboratory (NREL) at www.nrel.gov/publications.

Available electronically at SciTech Connect http:/www.osti.gov/scitech

Available for a processing fee to U.S. Department of Energy and its contractors, in paper, from:

U.S. Department of Energy
Office of Scientific and Technical Information
P.O. Box 62
Oak Ridge, TN 37831-0062
OSTI http://www.osti.gov
Phone: 865.576.8401
Fax: 865.576.5728
Email: reports@osti.gov

Available for sale to the public, in paper, from:

U.S. Department of Commerce
National Technical Information Service
5301 Shawnee Road
Alexandria, VA 22312
NTIS http://www.ntis.gov
Phone: 800.553.6847 or 703.605.6000
Fax: 703.605.6900
Email: orders@ntis.gov

Cover Photos by Dennis Schroeder: (left to right) NREL 26173, NREL 18302, NREL 19758, NREL 29642, NREL 19795.

NREL prints on paper that contains recycled content.

Grid Frequency Extreme Event Analysis and Modeling

Maria Folgueras, Erin Wenger, Anthony Florita, Kara Clark, and Vahan Gevorgian
National Renewable Energy Laboratory
Golden, CO, USA

***Abstract*—Sudden losses of generation or load can lead to instantaneous changes in electric grid frequency and voltage. Extreme frequency events pose a major threat to grid stability. As renewable energy sources supply power to grids in increasing proportions, it becomes increasingly important to examine when and why extreme events occur to prevent destabilization of the grid. To better understand frequency events, including extrema, historic data were analyzed to fit probability distribution functions to various frequency metrics. Results showed that a standard Cauchy distribution fit the difference between the frequency nadir and pre-fault frequency (f_{C-A}) metric well, a standard Cauchy distribution fit the settling frequency (f_B) metric well, and a standard normal distribution fit the difference between the settling frequency and frequency nadir (f_{B-C}) metric very well. Results were inconclusive for the frequency nadir (f_C) metric, meaning it likely has a more complex distribution than those tested. This probabilistic modeling facilitates more realistic modeling of grid faults.**

Keywords-frequency; voltage; extreme events; probabilistic

NOMENCLATURE

$\mathbf{f_A}$ – Avg. of freq. from -16s to 0s before an event [Hz] [17]
$\mathbf{f_B}$ – Avg. of freq. from 20s to 52s after an event [Hz] [17]
$\mathbf{f_C}$ – Freq. nadir; min. freq. achieved during a loss of gen. event [Hz] [17]
$\mathbf{f_{C-A}}$ – Difference between f_C and f_A ($f_C - f_A$) [Hz]
$\mathbf{f_{max}}$ – Max. freq. prior to a loss of gen. event [Hz] [3]
$\mathbf{\Delta f}$ – Freq. delta ($f_C - f_{max}$) [Hz] [3]
$\mathbf{T(0)}$ – NERC-defined point at which a min. freq. change of at least 5 mHz occurs within a 1s time span [Hz] [17]
$\mathbf{\Delta t}$ – Time duration of freq. event [s]
$\mathbf{t_c}$ – Time at which f_C occurs [hh:mm:ss]
$\mathbf{t_{max}}$ – Time at which f_{max} occurs [hh:mm:ss]
ROCOF – Rate of change of freq.; slope of the event [Hz/s]
H – Inertia coefficient [MW·s]
$\mathbf{FR_{Current}}$ – Measure of effectiveness of primary freq. response capabilities to correct freq. deviations during an event [MW/Hz] [15]
f_{B-C} – Difference between f_B and f_C ($f_B - f_C$) [Hz]

I. INTRODUCTION

The electric grid transmits and distributes electricity across the U.S. at a nominal frequency of 60 Hz [1]. Synchronous generators set the frequency and come equipped with primary control reserves [2]. These reserves, also known as primary frequency response (PFR), assist in recovering the grid frequency after it deviates from the nominal value sharply (i.e., the difference between the maximum and minimum event frequency exceeds 70 mHz in a 15-second rolling window) [3] or significantly (i.e., the frequency is less than 59.95 Hz or more than 60.05 Hz in the Western Interconnection) [4]. Secondary and tertiary frequency responses also act to correct frequency deviations to the nominal value (much like PFR), but they are delivered after PFR and during longer time periods [5]. Frequency deviations can result from an instantaneous loss of generation or load [6]. Frequency response controls are needed to prevent frequency deviation events.

Extreme frequency events are characterized "by non-linear responses, low probabilities, high consequences, and the potential for systems interaction that leads to catastrophic losses" [7]. They could be brought about by extreme weather, interrupting power generation and transmission, but also, in the near future, the impact of high penetrations of renewable power onto the grid. Renewable sources exacerbate challenges to frequency stability and grid reliability because of their variable and uncertain operation [8]. Renewable sources do not come equipped with synchronous generators or PFR capabilities [8], meaning that when large amounts of inverter-based renewable generation are brought onto the 60-Hz operating grid, PFR capabilities might be reduced unless the renewable power plants are equipped with special frequency responsive controls [9]. Instabilities in generation can cause extreme events such as underfrequency load-shedding, triggering under/overfrequency protection relays, and reaching the frequency nadir [1]. Reaching the frequency nadir can lead to cascading failures on the grid because at this point the grid frequency is no longer regulated and stabilized at its nominal value [10].

Issues of grid reliability have turned the focus of research to grid resilience during and after an extreme event. Generally, two factors affect infrastructure resilience after an extreme event: robustness and rapidity. Robustness is a measure of how much of the system remains functioning after an extreme event, and rapidity is a measure of how quickly the entire system can fully function again after the event [11]. The U.S. electric grid comprises countless power plants and millions of miles of transmission lines, thus it is the largest infrastructure in the world, and it can be categorized and studied in the vein of infrastructure

resilience. Extreme events greatly stress the grid, and must be understood to allow for the integration of larger amounts of renewable energy penetration. By studying previous extreme events, outage frequencies, and outage durations, probability models were developed to attempt to predict these events happening in the future. The results suggest that these models can be used by system operators to approximate the probability of future frequency events, to plan generation and load balancing accordingly, and to possibly prevent frequency events from occurring as often as they do on the present electric grid.

II. Data and Methodology

A. Description of Data

Electric frequency data collected at NREL's National Wind Technology Center (NWTC) was obtained, with date, time, and frequency, during an approximate 2-year time span. The monitoring system is a National Instruments model cDAQ-9171 chassis with a 9225 voltage measurement module (24-bit, 300 VRMS), and was plugged into a 110-V wall outlet and connected to a PC using a USB 2.0 cable (Figure 1) [12].

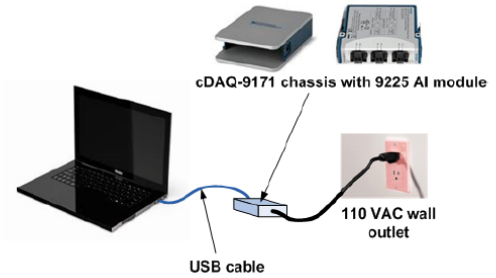

Figure 1. Frequency monitoring system used at the NWTC to collect frequency data for this project. Reprinted from [12].

Data were collected from August 1, 2014, until June 10, 2016, with occasional days of data missing because of unplanned device disconnections. The provided data were collected every 2 ms from August 1, 2014, to April 31, 2016, and collected every 1 ms from May 1, 2016 onward.

B. Data Validation

NWTC data were validated by comparing them to frequency event records provided by the North American Electric Reliability Corporation (NERC) [13]. At the time of the study, NERC had provided frequency event data only through March 31, 2016. For each frequency event recorded by NERC, the corresponding NWTC data were compared. The specific frequency decrease pattern before, during, and after the events were analyzed to determine a frequency event match. Events when frequency increased were ignored in this study; such events are not of interest as they represent a loss of load whereas this study focuses on loss of generation. In the subset of matched data, various frequency metrics were calculated from the NWTC data and compared to the corresponding NERC data. These metrics included f_A, f_B, f_C, and f_{C-A}. The metrics f_{max}, Δf, and $T(0)$ were also determined but not for comparison purposes (Figure 2) [14].

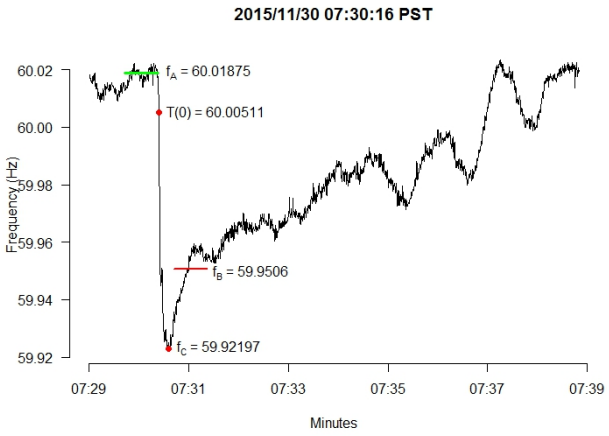

Figure 2. Graphical representation of frequency event on November 13, 2015, from NWTC data (verified with NERC records) [14]

After qualitative data analysis, a five-point moving average of the NWTC dataset was taken to smooth the data in an attempt to remove some of the variability and noise in the NWTC data that was not present in the NERC data. All previously mentioned values were again determined (f_A, f_B, f_C, f_{C-A}, f_{max}, Δf, and $T(0)$). This new five-point average dataset is referred to as the NWTC MA dataset. The percentage differences among the various NERC, NWTC, and NWTC MA values were calculated and used as comparison metrics (Table 1). The percentage differences between the NWTC and NWTC MA values were particularly important because they highlighted the impact of the applied five-point moving average on the data.

C. Calculation of Frequency Response Metrics

To calculate various frequency response metrics for each event recorded in the NWTC dataset, the time duration of the event (Equation 1) and the rate of change of frequency (Equation 2) were both determined.

$$\Delta t = t_C - t_{max} \quad (1)$$

$$ROCOF = \frac{\Delta f}{\Delta t} \quad (2)$$

The generation loss, ΔP, that occurred during each event was provided by NERC [12]. This gave enough information to calculate the inertia coefficient (Equation 3) [5].

$$H = \left|\frac{f_A \cdot \Delta P}{2 \cdot ROCOF}\right| \quad (3)$$

Finally, the frequency response as defined by NERC was calculated for each event (Equation 4) [15].

$$FR_{Current} = \frac{\Delta P}{f_A - f_B} \quad (4)$$

Various combinations of the calculated data were plotted as scatterplots to identify causal patterns (Table 2). Linear regressions were performed and R^2-values compared. An evaluation was made of how the number of frequency events varied during different time frames. The number of events per month in the studied time frame (August 1, 2014, to March 31, 2016) and the number of events per season in the studied time frame were analyzed.

TABLE I. DETERMINED OR CALCULATED METRICS USED IN DATA VALIDATION FOR EVENT ON NOVEMBER 13, 2015

	NERC	NWTC	% Δ b/w NERC and NWTC	NWTC MA	% Δ b/w NERC and NWTC MA	% Δ b/w NWTC and NWTC MA
f_A (Hz)	60.019	60.019	4.17e-04%	60.019	5.33e-04%	1.17e-04%
f_B (Hz)	59.950	59.951	1.00e-03%	59.951	9.84e-04%	1.67e-05%
f_C (Hz)	59.924	59.922	3.39e-03%	59.923	2.39e-03%	1.00e-03%
f_{C-A} (mHz)	-95.000	-96.780	-1.87e+00%	-96.110	-1.17e+00%	-6.92e-01%
f_{max} (Hz)	NA	60.020	NA	60.019	NA	1.08e-03 %
Δf (mHz)	NA	-97.700	NA	-96.450	NA	-1.28e+00%
$T(0)$ (Hz)	NA	60.005	NA	60.004	NA	2.57e-03%

TABLE II. SCATTERPLOTS USED TO ANALYZE CALCULATED DATA

Scatterplots
H vs. ΔP
H vs. Δt
NERC f_C vs. Δt
NWTC f_C vs. Δt
NWTC MA f_C vs. Δt

III. ANALYSIS

A. Linear Regression

An acceptable linear relationship was found between the calculated H-values and Δt from the NWTC data (Table 3); i.e., an R^2-value of 0.7932. It should be noted a limited amount of data used: only 67 events, and of those 67 events, 22 did not have ΔP information from NERC, and 1 had too much noise in the NWTC data to properly analyze the event. As a result, only 44 events could be used in linear regression analysis. More data could help strengthen the R^2-value and thus the linear correlation between H and Δt. It is also clear that the H and Δt R^2-value suggests a stronger linear correlation between H and Δt when compared to the other R^2-values obtained in this analysis (Table 3).

TABLE III. LINEAR REGRESSION ANALYSIS OF VARIOUS SCATTERPLOTS

Scatterplot	R^2-value	Slope of Regression Line	Intercept of Regression Line
H vs. ΔP	0.0023	185.72	2e+06
H vs. Δt	0.7932	223636	231197
NERC f_C vs. Δt	0.1094	0.0026	59.891
NWTC f_C vs. Δt	0.1246	0.0028	59.885
NWTC MA f_C vs. Δt	0.1125	0.0027	59.888

A positive linear correlation between H and Δt means that as the inertia coefficient of the system (H) increases, the time duration of the event (Δt) also increases (Figure 3). This is reasonable because H and Δt are directly proportional through the combination of (2) and (3):

$$H = \left|\frac{f_A \cdot \Delta P}{2 \cdot ROCOF}\right| = \left|\frac{f_A \cdot \Delta P}{2 \cdot (\frac{\Delta f}{\Delta t})}\right| = \left|\frac{f_A \cdot \Delta P \cdot \Delta t}{2 \cdot \Delta f}\right| \quad (5)$$

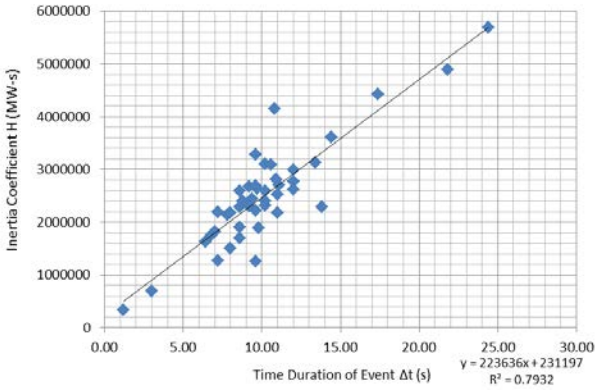

Figure 3. Inertia coeff. H vs. time duration of event Δt for NWTC data

B. Variation of Number of Events over Time

A correlation was found to exist between the number of events and the month in which they occurred. There seems to be a cyclical pattern: more events occur in the spring (March, April, May) and fall (Sept., Oct., Nov.) (Figure 4).

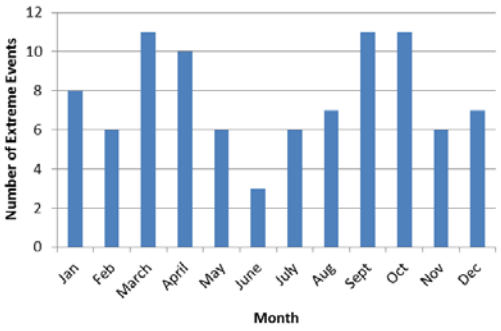

Figure 4. Number of frequency events per month in the studied August 1, 2014, to March 31, 2016, time frame

Results suggest a relationship between extreme events and seasonality (Figure 4). More events occur during the "shoulder" or off-peak spring and fall months than during the peak summer and winter months (Figure 5). An explanation for this pattern might be that grid operators take advantage of off-peak seasons to commission facility maintenance, replacement, or new construction. As a result, fewer generators are online and supplying power to the grid during these seasons. A smaller pool of online generators lowers the inertia of the grid, making it more susceptible to instability with a sudden loss of generation or load [16].

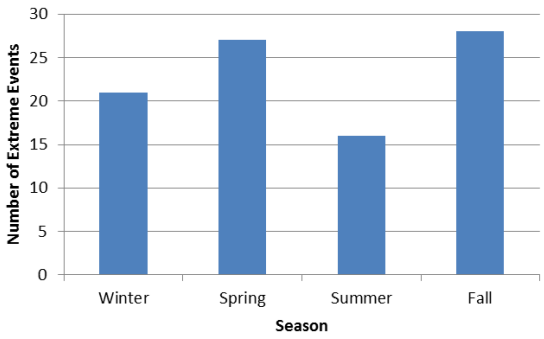

Figure 5. Number of frequency events per season in the studied August 1, 2014, to March 31, 2016, time frame

C. *Probability Distribution Functions*

From the density histogram of the normalized f_{C-A} metric, a standard Cauchy distribution was determined to most closely fit the empirical density function of the dataset (Table 4, Figure 6).

TABLE IV. PARAMETERS OF CAUCHY DISTRIBUTION FOR NORMALIZED AND ORIGINAL f_{C-A} DATASETS

Dataset	μ	σ	Interval of μ±1σ
Normalized	0	1	(-1, 1)
Original	-86.59831 mHz	37.41474 mHz	(-124.013 mHz, -49.18357 mHz)

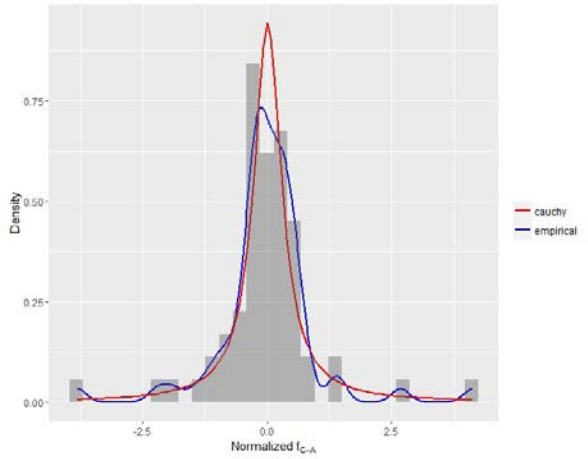

Figure 6. Density of normalized NWTC f_{C-A} with overlaid empirical and standard Cauchy distributions

This means that 68.2% of the normalized f_{C-A} observations is contained within the interval (-1,1) and that 68.2% of the original f_{C-A} observations is contained within the interval (-124.0 mHz, -49.2 mHz).

From the density histogram of the normalized f_B metric, results were inconclusive in fitting a distribution to the empirical density function of the dataset (Figure 7). Consequently, the dataset likely has a more complex distribution than those tested.

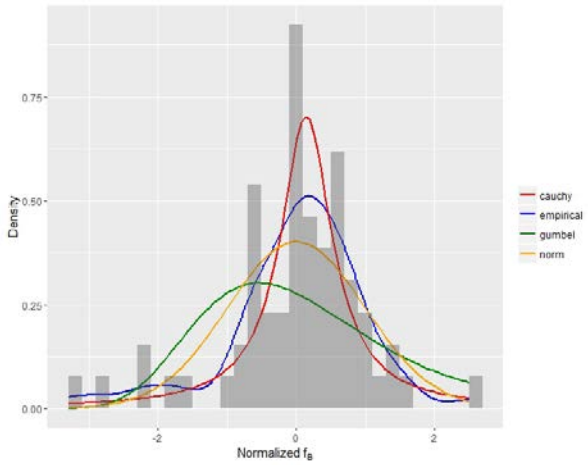

Figure 7. Density of normalized NWTC f_B with overlaid empirical, standard Cauchy, standard Gumbel, and standard normal distributions

From the density histogram of the normalized f_C metric, a standard Cauchy distribution was determined to most closely fit the empirical density function of the dataset (Table 5, Figure 8).

TABLE V. PARAMETERS OF CAUCHY DISTRIBUTION FOR NORMALIZED AND ORIGINAL f_C DATASETS

Dataset	μ	Σ	Interval of μ±1σ
Normalized	0	1	(-1, 1)
Original	59.91567 Hz	40.09544 mHz	(59.87557 Hz, 59.95576 Hz)

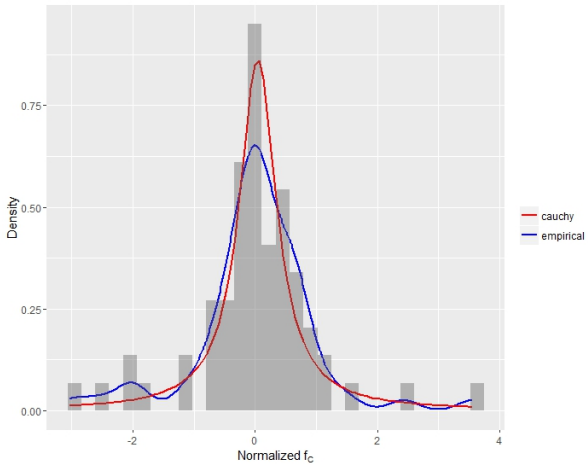

Figure 8. Density of normalized NWTC f_C with overlaid empirical and standard Cauchy distributions

Assuming a standard normal distribution, 68.2% of the f_C observations are contained within the interval (-1,1). As such, 68.2% of the original f_C observations are contained within the interval (59.87557 Hz, 59.95576 Hz).

From the density histogram of the normalized f_{B-C} metric, a standard normal distribution was determined to best fit the empirical density function of the dataset (Table 6, Figure 9).

TABLE VI. PARAMETERS OF NORMAL DISTRIBUTION FOR NORMALIZED AND ORIGINAL f_{B-C} DATASETS

Dataset	μ	Σ	Interval of μ±1σ
Normalized	0	1	(-1, 1)
Original	31.78 mHz	15.98 mHz	(15.80 mHz, 47.76 mHz)

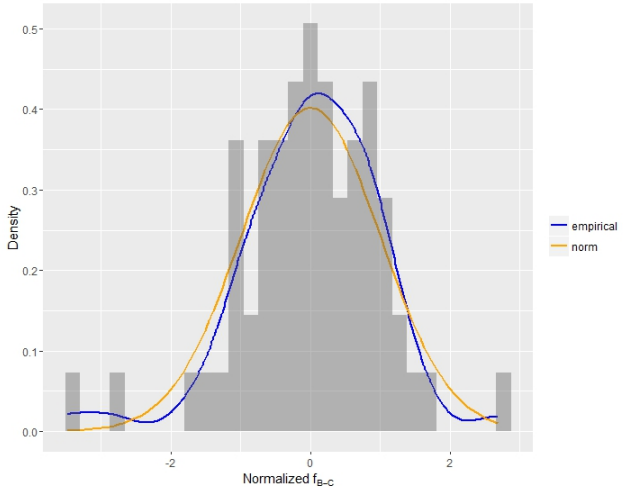

Figure 9. Density of normalized NWTC f_{B-C} with overlaid empirical and standard normal distributions

Again, 68.2% of the normalized f_{B-C} observations are contained within the interval (-1,1), and 68.2% of the original f_{B-C} observations are contained within the interval (15.80 mHz, 47.76 mHz).

Q-Q and P-P plots of both the normalized and original f_{B-C} data supported the assertion that a standard normal distribution fits the metric very well (Figure 10). This suggests that the quantiles of the empirical distribution match the quantiles of the theoretical distribution for the normalized f_{B-C} data well. Most points appear to lie close to the reference line, with greater deviations occurring at both tails. These deviations are caused by the few outliers in the normalized f_{B-C} dataset, which correspond to outliers in the original f_{B-C} dataset (Figure 11). Most of the data in the original f_{B-C} dataset are clustered in the range from 4 mHz to 58 mHz, though three outlier points occur at f_{B-C} values of -23.97 mHz, -13.81 mHz, and 74.61 mHz.

These outliers represent frequency events of greater "extremity," indicating events that have larger frequency deviations from the nominal value. Fewer events of greater extremity are expected because adequate reserves are online and providing inertia to the grid. These reserves include generators that provide PFR, secondary frequency response, and tertiary frequency response to arrest frequency deviations quickly in most instances of a loss of generation or load.

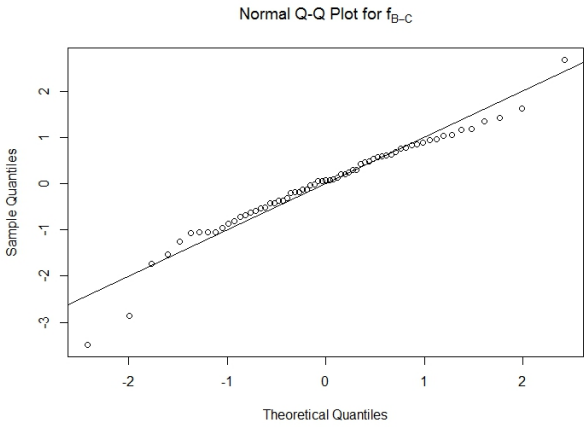

Figure 10. Q-Q plot for normalized f_{B-C} data with overlaid reference line $y = x$

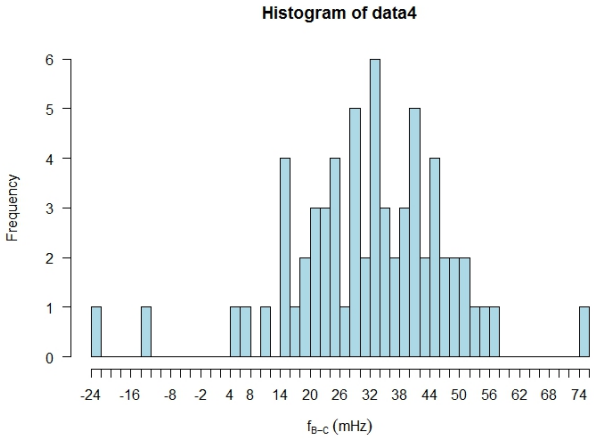

Figure 11. Figure 11. Histogram of original f_{B-C} dataset

With μ = 31.77815 mHz and σ = 15.97807 mHz, the original f_{B-C} data have the reference line $y = 0.03177815x + 0.01597807$ for a Q-Q plot, and the plotted points again lie closely (Figure 12). This suggests that the quantiles of the empirical distribution closely match the quantiles of the theoretical distribution for the original f_{B-C} data. Similar to Figure 10, most points appear to lie closely to the reference line, with greater deviations occurring at the t. The deviations correspond to the same outliers previously discussed from the original f_{B-C} dataset (Figure 11). In fact, Figure 10 and Figure 12 are identical, except for the scale on the y-axis. This is significant because it suggests that a standard normal distribution is a good fit for the original f_{B-C} data, not solely the normalized f_{B-C} data.

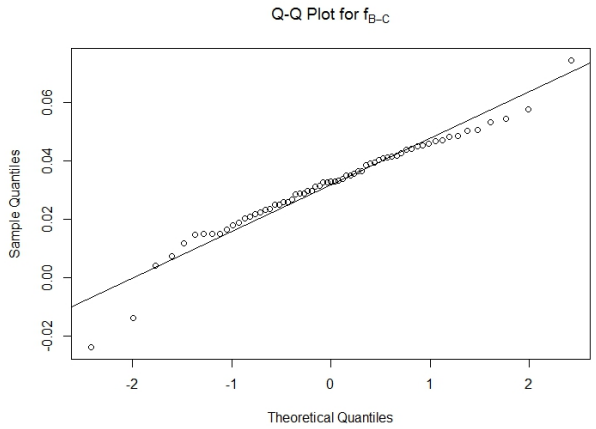

Figure 12. Q-Q plot for original f_{B-C} data with overlaid reference line $y = 0.03177815x + 0.01597807$

The normalized f_{B-C} data considered in a P-P plot (Figure 13) suggests that the empirical cumulative distribution function (CDF) matches the theoretical CDF for the normalized f_{B-C} data well. The middle points appear to lie closely to the reference line, with greater deviations occurring at the tails of the dataset. These deviations correspond to the three outliers previously analyzed in the original f_{B-C} data (Figure 11).

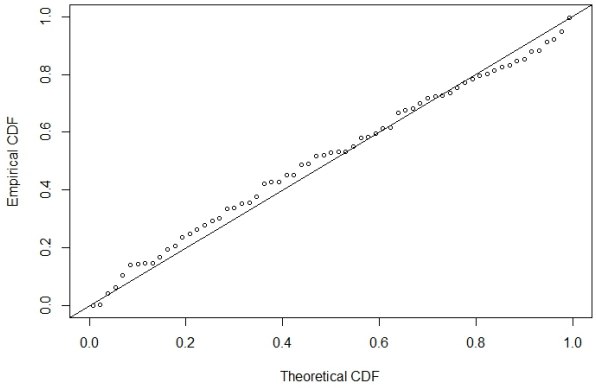

Figure 13. P-P plot for normalized f_{B-C} with overlaid reference line $y = x$

IV. Conclusions & Recommendations

Understanding past frequency events will help lower the risks associated with increased levels of renewable generation onto the grid. Using existing frequency event data, probability models of various frequency metrics have been developed. These models help assess frequency stability and grid reliability. The models suggest that more frequency events tend to be of a smaller extremity (i.e. center of the distributions) but that some events are of greater extremity (i.e. outliers or the tails of the distribution).

Modeling improvements can be made by having more data available for fitting. The data used in this analysis contained only 65 data points. Future work could include fitting probability density functions to the same frequency metrics but for a larger number of frequency events. Frequency event data have been collected at the NWTC since June 16, 2011, and data collection is ongoing.

Acknowledgment

This work was supported by the U.S. Department of Energy under the Grid Modernization Laboratory Consortium through Contract No. DE-AC36-08-GO28308 with the National Renewable Energy Laboratory (NREL). M.F. and E.W. would like to thank the SULI program.

References

[1] E. Ela, V. Gevorgian, A. Tuohy, B. Kirby, M. Milligan, and M. O'Malley, "Market designs for the primary frequency response ancillary service—Part I: Motivation and design," IEEE Trans. Power Syst. vol. **29**, pp. 421–431, 2014.

[2] D. Weisser and R. S. Garcia, "Instantaneous wind energy penetration in isolated electricity grids: concepts and review," Renewable Energy **30**, pp. 1299–1308, 2005.

[3] NERC, CERTS, and Electric Power Group, "Delta frequency detection methodology," Frequency Event Detection Methodology, Oct. 2012, (July 5, 2016).

[4] NERC, "Procedure for ERO support of frequency response and frequency bias setting standard," BAL-003-1 Frequency Response & Frequency Bias Setting Standard, Nov. 30, 2012, (July 5, 2016).

[5] S. Sharma, S. Huang, and N. Sarma, presented at the 2011 IEEE Power and Energy Society General Meeting, San Diego, CA, 2011 (published).

[6] J. H. Eto, J. Undrill, P. Mackin, R. Daschmans, B. Williams, B. Haney, R. Hunt, J. Ellis, H. Illian, C. Martinez, M. O'Malley, K. Coughlin, and K. Hamachi LaCommare, "Use of frequency response metrics to assess the planning and operating requirements for reliable integration of variable renewable generation," eScholarship, 2011.

[7] S. E. Chang, T. L. McDaniels, J. Mikawoz, and K. Peterson, "Infrastructure failure interdependencies in extreme events: power outage consequences in the 1998 Ice Storm," Nat. Hazards **41**, 337–358, 2006.

[8] E. Ela, V. Gevorgian, A. Tuohy, B. Kirby, M. Milligan, and M. O'Malley, "Market designs for the primary frequency response ancillary service—Part II: Case studies," IEEE Trans. Power Syst. **29**, 432–440, 2014.

[9] V. Akhmatov, "The mutual effects of grid and wind turbine voltage stability control," Wind Engineering **25**, 367–371, 2001.

[10] H. Bevrani, A. Ghosh, and G. Ledwich, "Renewable energy sources and frequency regulation: survey and new perspectives," IET Renew Power Gen **4**, 438–457, 2010.

[11] T. McDaniels, S. Chang, D. Cole, J. Mikawoz, and H. Longstaff, "Fostering resilience to extreme events within infrastructure systems: Characterizing decision contexts for mitigation and adaptation," Global Environmental Change **18**, 310–318 (2008).

[12] E. Ela, V. Gevorgian, P. Fleming, Y.C. Zhang, M. Singh, E. Muljadi, A. Scholbrook, J. Aho, A. Buckspan, L. Pao, V. Singhvi, A. Tuohy, P. Pourbeik, D. Brooks, and N. Bhatt. Active Power Controls from Wind Power: Bridging the Gaps (Tech. Rep.). Golden, CO: National Renewable Energy Laboratory, 2014, p. 154.

[13] NERC, Resources Subcommittee, May 18, 2016, (July 20, 2016).

[14] CERTS and Electric Power Group. Eastern, WECC, ERCOT and Quebec Frequency Events' Data Summary and Corresponding Frequency Plots for November 2015 (Tech. Rep.). 2015, p. 13.

[15] NERC. Essential Reliability Services Task Force Measures Framework Report (Tech. Rep.). Atlanta, GA: 2015, p. 139.

[16] R. Baldick, B. Chowdhury, I. Dobson, Z. Dong, B. Gou, D. Hawkins, H. Huang, M. Joung, D. Kirschen, F. Li, J. Li, Z. Li, C. Liu, L. Mili, S. Miller, R. Podmore, K. Schneider, K. Sun, D. Wang, Z. Wu, P. Zhang, W. Zhang, and X. Zhang, presented at the 2008 IEEE Power and Energy Society General Meeting, Pittsburgh, PA, 2008 (published).

[17] CERTS, "FRSDT Action Item: Define how and when to use 2 years of event data in addition to the 1 year currently in the draft standard," 2012, p. 3